

# Structural and dielectric properties of epitaxial $\text{Ba}_{0.6}\text{Sr}_{0.4}\text{TiO}_3$ thin films grown on Si substrates with thin SrO buffer layers

Hyun-Suk Kim · Tae-Seon Hyun · Ho-Gi Kim ·  
Tae-Soon Yun · Jong-Chul Lee · Il-Doo Kim

Received: 27 November 2006 / Accepted: 27 April 2007 / Published online: 17 May 2007  
© Springer Science + Business Media, LLC 2007

**Abstract** (100) epitaxial  $\text{Ba}_{0.6}\text{Sr}_{0.4}\text{TiO}_3$  (BST) thin films were grown on Si substrates using a 9 nm thick SrO buffer layer. The phase shifter fabricated on BST films grown on a SrO buffered Si substrate showed a larger figure of merit (FOM) of 24.7°/dB as a result of improving the phase tuning while retaining an appropriate insertion loss compared to that (15.3°/dB) for the BST/MgO structure. This work demonstrates that a thin SrO buffer layer plays an important role in the successful integration of BST-based microwave tunable devices onto Si wafers.

**Keywords** SrO · BST · Phase shifter · Si integration · Buffer layer

## 1 Introduction

(Ba,Sr)TiO<sub>3</sub> (BST) thin films have been widely studied for their potential application in tunable microwave devices such as tunable filters, tunable oscillators, and phase shifters. They are useful due to the large variation of dielectric constant in ferroelectric thin films through the application of a dc electric field at room temperature [1]. A nonlinear dependence of the dielectric permittivity is a feature of ferroelectric materials. For applications of frequency-agile devices, it is highly desirable to have as large a dielectric permittivity change ratio [dielectric tunability =  $(\epsilon_{\max} - \epsilon_{\min})/\epsilon_{\max}$ , where  $\epsilon_{\max}$  and  $\epsilon_{\min}$  are the maximum and minimum value of permittivity, respectively] and as low a dielectric loss as possible. To date, there have been extensive studies to increase the dielectric tunability and to reduce the dielectric loss of BST thin films grown on single crystal substrates such as LaAlO<sub>3</sub> [2] and MgO [3], among others, however, the use of these substrates is associated with major drawbacks from an industrial point of view due to their high cost and small-sized geometry [4, 5]. Furthermore, the mounting techniques of components during the fabrication of hybrid microwave-integrated circuits are not simple. It is of significant interest to integrate BST-based high-frequency devices onto Si substrates, as integrated device technologies largely rely on the Si process with its inherent low cost, large area, and high-volume production.

However, it is difficult to fabricate high-quality BST thin films directly onto Si substrates as a native oxide is easily formed on the Si surface during the requisite high-temperature BST deposition process [6]. In order to solve this problem, suitable oxide buffer layers with low dielectric loss and high resistivity characteristics should be

---

H.-S. Kim  
Department of Materials Science and Engineering,  
Massachusetts Institute of Technology,  
Cambridge, MA 02139, USA

T.-S. Hyun · H.-G. Kim  
Department of Materials Science and Engineering,  
Korea Advanced Institute of Science and Technology,  
Daejeon 305-701, Republic of Korea

T.-S. Yun · J.-C. Lee  
RFIC Research and Education Center, Kwangwoon University,  
447-1 Wolgye-dong, Nowon-gu,  
Seoul 139-703, Republic of Korea

I.-D. Kim (✉)  
Optoelectronic Materials Research Center,  
Korea Institute of Science and Technology,  
P.O. Box 131, Cheongryang,  
Seoul 130-650, Republic of Korea  
e-mail: idkim@kist.re.kr

incorporated between the top BST films and Si substrates in order to prevent SiO<sub>2</sub> formation and to control the orientation and quality of the BST films. Moreover, the oxide buffer layers should be thin enough to offer moderate operating voltages, as significant power losses through Si substrates may be generated due to the low dielectric constants of given buffer layers. Thus far, considerable efforts have been made to grow epitaxial BST films on relatively thick buffer layers (>20 nm) [7, 8] or double buffer layers (e.g., Bi<sub>4</sub>Ti<sub>3</sub>O<sub>12</sub>/YSZ, CeO<sub>2</sub>/YSZ) [9, 10]. However, few articles have been published on ultra-thin SrO buffered BST thin films on tunable dielectric properties in a microwave frequency regime. In this paper, the role of an ultra-thin SrO buffer layer to obtain high-quality BST thin films epitaxially grown on high-resistivity Si substrates is reported. The microwave dielectric properties of BST/SrO/Si structure are compared with those of (100) epitaxial BST/MgO which has been extensively studied as potential tunable element. The successful characterization of Si-integrated BST phase shifters with the desired performance using 9 nm thick SrO buffer layers is discussed.

## 2 Experimental procedures

BST/SrO heterostructures were prepared on p-type Si (100) substrates with a high resistivity of 10 kΩcm by a pulsed-laser deposition (PLD) system using a KrF excimer source ( $\lambda=248$  nm, Lambda Physik COMPEX 205). Sintered pellets of Ba<sub>0.6</sub>Sr<sub>0.4</sub>TiO<sub>3</sub> and SrO<sub>2</sub> were used as targets. Before the deposition of the SrO layers on the Si (100) substrates, the Si wafers were etched using a 10% HF solution for 1 min in order to remove the native oxide layers. The laser energy used for both the SrO and BST films was 100 mJ/pulse. SrO and BST films were continuously in-situ deposited at a substrate temperature ( $T_s$ ) of 700°C in order to prevent surface contamination of the SrO films during a vacuum-break. The repetition rate for the growth of the SrO thin films and the distance between the target and the substrate (T-S) were 1 Hz and 30 mm, respectively. The oxygen pressure was maintained at a fixed value in a range from  $3 \times 10^{-6}$  to  $1 \times 10^{-5}$  Torr for each deposition. The thickness of the SrO layer was varied from 5 to 40 nm. BST thin films were subsequently deposited at a repetition rate of 10 Hz, a T-S of 70 mm, and an O<sub>2</sub> pressure of  $10^{-2}$  Torr. After the in-situ deposition, the BST films were cooled to room temperature in an oxygen pressure of 5 Torr to preserve the oxygen content in the films during the cooling procedure. The crystal structures of the BST and SrO films were investigated by a  $\theta-2\theta$ ,  $\omega$ -scan (rocking curve), and pole-figure measurements using X-ray diffractometry (XRD, Rigaku D/MAX-RC) excited with CuK $\alpha$  radiation. The microstructures and surface morphol-

ogies of the films were characterized by scanning electron microscopy (SEM, Philips XL 30SFEG). In order to investigate the microwave tunable properties of the BST films, bilateral interdigital coplanar waveguide (BI-CPW) phase shifter circuits were fabricated on BST films (0.5  $\mu$ m thick, deposited onto SrO/Si and MgO substrates) by standard photolithography and a lift-off process. A CPW center conductor and gap dimensions of 100 and 80  $\mu$ m were used. The length of the signal line was chosen to be 8.2 mm. Narrow transverse slits with a length of 500  $\mu$ m were inserted into the center signal line to provide higher phase shifting capability. Au (25 nm)/Ag (1.45  $\mu$ m)/Ti (25 nm) metal layers of 1.5  $\mu$ m thick were deposited using dc magnetron sputtering to produce the CPW electrodes. In order to compare the dielectric properties of the BST films grown on SrO/Si and MgO substrates at 5 GHz, an interdigital capacitor (IDC) with a total of six fingers, an overlap length of 300  $\mu$ m, a finger width of 10  $\mu$ m, and a finger gap of 5  $\mu$ m was fabricated. The microwave properties of the BST thin films were measured using a HP 8510C network analyzer equipped with a ground-signal-ground probe in a frequency range from 1 to 12 GHz at room temperature. A dc bias voltage was applied to the device through external bias tees in order to protect the network analyzer.

## 3 Results and discussion

Figure 1 shows the XRD patterns of the SrO template layers with a thickness of 40 nm as a function of the oxygen pressure ranging from  $1 \times 10^{-5}$  to  $6 \times 10^{-6}$  Torr and 100 nm-thick BST films deposited on SrO(40 nm)/Si substrates. The SrO template films exhibited highly (200)

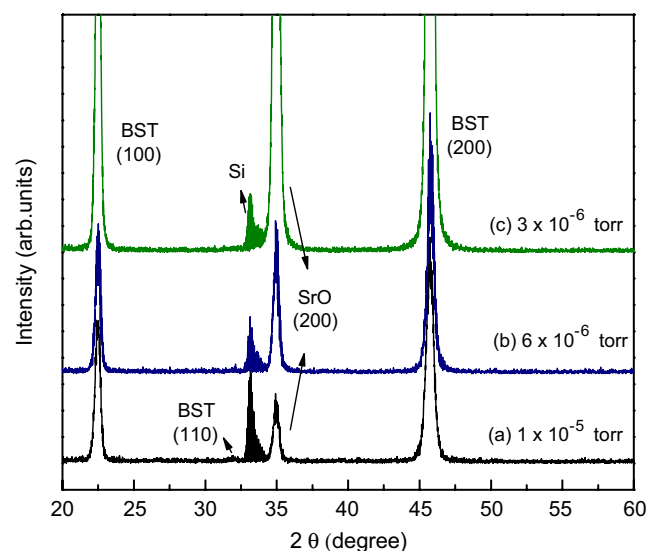


**Fig. 1** XRD patterns of 100 nm-thick BST films deposited on SrO (40 nm)/Si substrates as a function of O<sub>2</sub> pressure for SrO layer

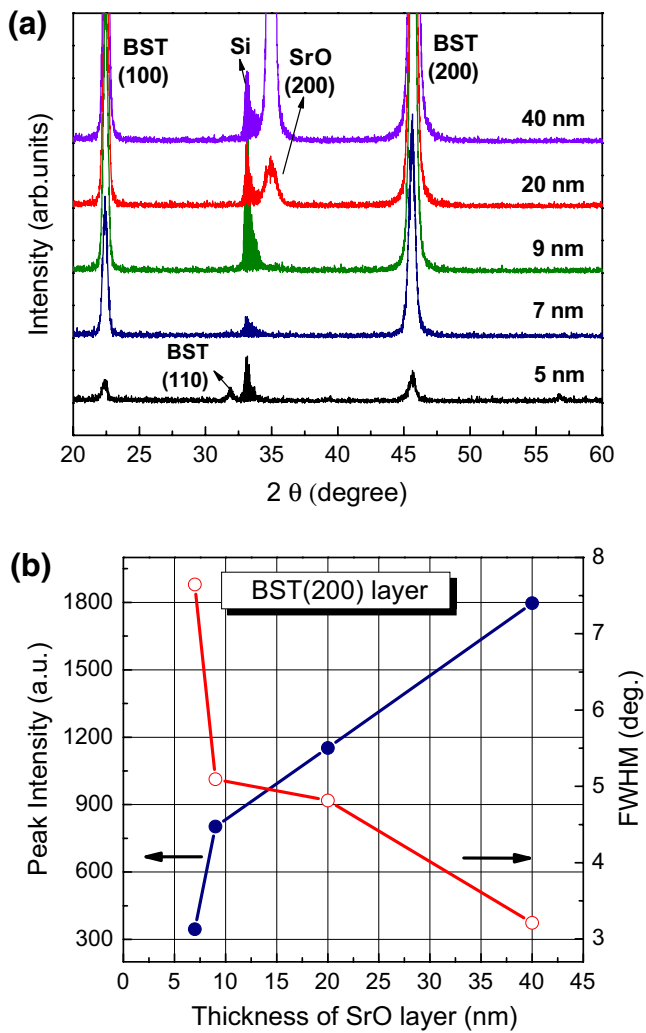


**Fig. 2** (a) XRD patterns of 100 nm-thick BST thin films deposited on SrO buffer layers of 5 nm, 7 nm, 9 nm, 20 nm, and 40 nm thickness. (b) Dependence of SrO thickness on intensities of BST (200) peak, and the full width at half maximum of BST (200) peak in XRD

preferred orientation with a single phase. The SrO (200) orientation may be promoted as a consequence of the structural match between SrO and the Si substrate with a small misfit of  $-5.5\%$  along the SrO  $\langle 010 \rangle //$  Si  $\langle 010 \rangle$  in SrO (100)/Si (100) [11]. As the oxygen pressure was decreased from  $1 \times 10^{-5}$  to  $6 \times 10^{-6}$  Torr, the intensities of the SrO (200) diffraction peaks slightly increased. With a further decrease the ambient oxygen pressure to  $3 \times 10^{-6}$  Torr, the peak intensities largely increased, indicating that the optimized oxygen pressure for the growth of high quality SrO films is  $3 \times 10^{-6}$  Torr. These results are ascribed to the interface improvement through the suppression of the degradation of SrO crystallinity, which can be induced by the formation of native oxide on the Si substrate at a high oxygen pressure ( $>1 \times 10^{-5}$  Torr) during the growth of the SrO film. As shown in Fig. 1(a), a BST films grown on SrO template layers deposited at an oxygen pressure of  $1 \times$

$10^{-5}$  Torr showed a (110) diffraction peak. The (110) diffraction peak disappeared in the BST films grown on SrO template layers deposited below  $6 \times 10^{-6}$  Torr. This result exhibits that the crystallinity of the SrO film improves with a decrease in the oxygen partial pressures, further indicating that high-quality SrO buffer layers can lead to a higher quality of BST films. Figure 2(a) shows XRD patterns of 100 nm-thick BST thin films deposited on SrO buffer layers with various thicknesses. The oxygen pressure for the growth of the SrO films was fixed at  $3 \times 10^{-6}$  Torr. As shown in Fig. 2(a), the BST films deposited on 5 nm-thick SrO films exhibited a polycrystalline nature due to the non-uniform island-like coverage of the SrO films. Therefore, SrO films with a thickness less than 5 nm cannot serve as a buffer layer. In contrast, the BST films grown on SrO buffer layers with a thickness above 7 nm showed an epitaxial relationship with Si (100), having a BST (100) and SrO (200) phase alone. SrO (200) phase was clearly observed in the film above 20 nm thickness. This result indicates that the crystallinity of SrO film improves as the SrO thickness increases. Figure 2(b) shows the variations of the peak intensities and the full width at half maximum (FWHM) values of the BST (200) diffraction peak as a function of the thickness of the SrO buffer layers. The FWHM for the (200) reflection of BST films on SrO buffer layers varied from 3.21 to 7.65. BST films grown on 40 nm thick SrO buffer layers exhibited the highest peak intensities and the lowest FWHM value. This result shows that the crystallinity of the BST films improved as the SrO thickness increased. However, for BST films grown on a SrO (40 nm thickness)/Si substrate, the BST films were found to have cracked after a long exposure in air due to the volume expansion by

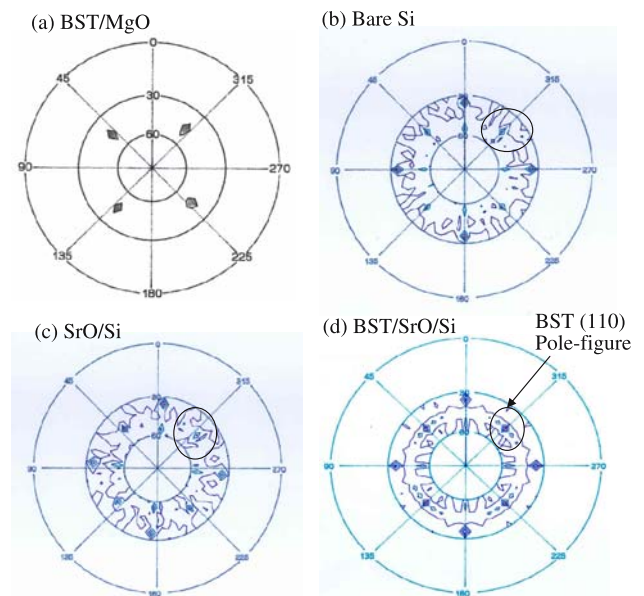


**Fig. 3** Pole figures for (a) BST/MgO, (b) bare Si substrate, (c) SrO/Si, and (d) BST/SrO/Si



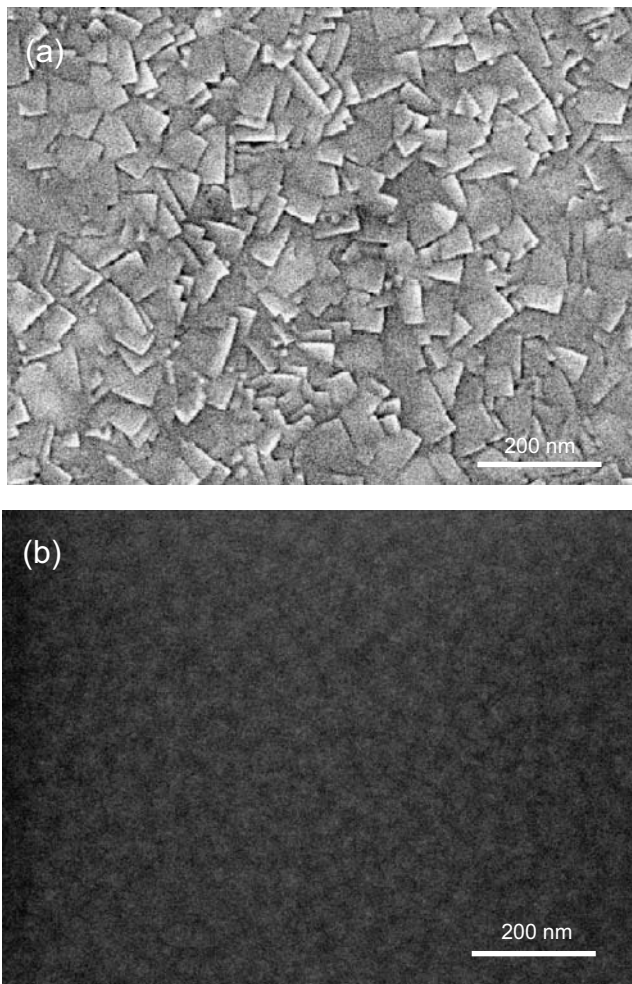


**Fig. 4** Surface SEM images of BST films with a thickness of 500 nm grown on (a) SrO buffered Si substrate and (b) MgO substrates

the formation of  $\text{SrCO}_3$  in the SrO buffer layer [12]. Therefore, SrO films with an appropriate thickness, in this case 9 nm, should be used as a buffer layer. In order to investigate the quality of the in-plane alignment, we carried out pole-figure measurement. Figure 3 shows X-ray pole figure of BST layer grown on MgO and SrO/Si substrates. As shown in Fig. 3(a), discrete diffraction spots with a fourfold symmetry were clearly observed when a BST (110) plane was used as a diffraction plane. This result indicates that the BST films have an epitaxial relationship with MgO substrate. SrO films grown on Si substrate didn't show any concentric ring due to very thin film thickness of 9 nm as shown in Fig. 3(b) and (c), similar epitaxial relationship was observed in BST films grown on SrO/Si substrate in Fig. 3(d) although very small deviation in concentric rings was incorporated. Thus, it is noted that the epitaxy in BST films on Si should be attributed to the lattice matching by using SrO templates as well as the prevention of the reaction with the substrates. In particular, these results are well matched with our earlier TEM results which showed an epitaxial relation-

ship:  $(100)_{\text{BST}}// (100)_{\text{Si}}$  and  $(111)_{\text{BST}}// (111)_{\text{Si}}$  in selected area diffraction pattern (SADP) of BST/SrO/Si [13].

Figures 4(a) and (b) show surface SEM images of 500 nm-thick BST films deposited onto SrO-buffered Si and MgO substrates, respectively. Both BST layers exhibited a uniform matrix of dense grains. In particular, larger grain growth was observed in the BST film grown on the SrO-buffered Si substrate; in comparison to the small-sized round-shaped grains ( $\sim 40$  nm) of the BST films grown on the MgO substrate. The BST film grown on the SrO/Si substrate showed a higher dielectric constant ( $\epsilon_r \sim 1,345$ ) compared to that ( $\epsilon_r \sim 1,097$ ) of the BST film deposited on a MgO substrate [13]. There are several possible explanations for increased dielectric constant of the BST/SrO/Si structure. First, the good lattice matching between the BST and SrO buffer layer is considered to assist in eliminating interface defects, leading to high-quality BST films. Second, the larger grain size distributions of the BST films grown on SrO/Si substrates are likely the source of the increased dielectric constant. Further studies should be conducted in order to clarify the dielectric behaviors. In order to demonstrate the advantages of epitaxial BST films grown on SrO-buffered Si substrates as tunable elements, CPW phase shifters were fabricated and characterized at room temperature at a frequency of 12 GHz. Figure 5 shows the differential phase shift for the CPW phase shifter based on BST/SrO/Si and BST/MgO structures as a function of applied dc bias voltages up to 50 V at 12 GHz. The measured differential phase shifts were 56.7 and 35.3° for BST/SrO/Si and BST/

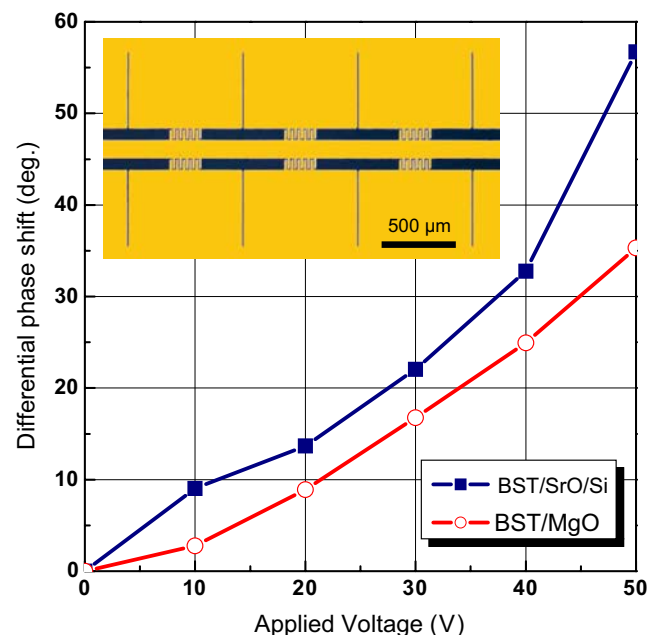


**Fig. 5** Differential phase shift as a function of dc bias voltage for BST/SrO/Si and BST/MgO structures at 12 GHz. Inset shows a schematic layout of the CPW phase shifter

MgO, respectively. These results correspond to phase shifts per applied voltage of 1.13 and 0.71 °/V for BST/SrO/Si and BST/MgO, respectively. This demonstrates that the (100) oriented BST/SrO/Si film exhibited better phase shifting capabilities compared to the (100) oriented BST/MgO structure. This result is mainly attributed to the larger dielectric constant of BST films ( $\epsilon_r \sim 1,345$ ) grown on an SrO/Si substrate compared to that of BST films ( $\epsilon_r \sim 1,097$ ) grown on MgO substrates [13]. The measured insertion loss ( $S_{21}$ ) at 12 GHz with a dc bias voltage of 0 V was 2.3 dB, for both BST/SrO/Si and BST/MgO. The figure of merit (FoM) of a phase shifter is defined by the differential phase shift ( $\Delta\phi$ ) divided by the maximum insertion loss (I.L.) for zero voltage. Therefore, FoM which can be given by  $\text{FoM} = \Delta\phi/\text{I.L.}$ , determines the utility of tunable dielectric films for device application. At a measured frequency of 12 GHz, the phase shifter fabricated on a BST film grown on a SrO buffered Si substrate showed a comparatively large FoM of 24.7°/dB as a result of improving the phase tuning while retaining an appropriate insertion loss. In comparison, a FoM of only 15.3°/dB was obtained for the BST/MgO structure.

#### 4 Conclusions

Epitaxial BST films with a (100) orientation were successfully deposited onto Si substrates using pulsed-laser deposited SrO films as template layers. The optimum conditions for the SrO buffer layers for BST epitaxial growth are a deposition temperature of 700°C, an O<sub>2</sub> pressure of  $3 \times 10^{-6}$  Torr, and a thickness of 9 nm. A coplanar waveguide phase shifter using a BST/SrO/Si structure showed a greater phase shifting capability compared to epitaxial BST films grown on MgO substrates. This result is mainly attributed to the larger dielectric constant of BST films ( $\epsilon_r \sim 1,345$ ) grown on SrO/Si

substrates compared to that of BST films ( $\epsilon_r \sim 1,097$ ) grown on MgO substrates. The figure of merit of the CPW phase shifter at 12 GHz was 24.7°/dB for a BST film grown on a SrO buffered Si substrate, while it was 15.3°/dB for a BST film grown on a MgO single crystal substrate. This work demonstrates that the use of a thin SrO buffer layer offers potential for the development of Si-integrated BST frequency agile devices.

**Acknowledgement** This work was supported by KIST independent project of one of the authors (I.D.K.).

#### References

1. I.D. Kim, H.L. Tuller, H.S. Kim, J.S. Park, *Appl. Phys. Lett.* **85**, 4705 (2004)
2. C.L. Chen, H.H. Feng, Z. Zhang, A. Brazdeikis, Z.J. Huang, W.K. Chu et al., *Appl. Phys. Lett.* **75**, 412 (1999)
3. W. Chang, J.S. Horwitz, A.C. Carter, J.M. Pond, S.W. Kirchoefer, C.M. Gilmore et al., *Appl. Phys. Lett.* **74**, 1033 (1999)
4. M.W. Cole, P.C. Joshi, M. Ervin, M. Wood, R. L. Pfeffer, *J. Appl. Phys.* **92**, 3967 (2002)
5. M.W. Cole, W.D. Nothwang, J.D. Demaree, S. Hirsch, *J. Appl. Phys.* **98**, 024507 (2005)
6. H.S. Kim, H.G. Kim, I.D. Kim, K.B. Kim, J.C. Lee, *Appl. Phys. Lett.* **87**, 212903 (2005)
7. S.Y. Hou, J. Kwo, R.K. Watts, J.Y. Cheng, D.K. Fork, *Appl. Phys. Lett.* **67**, 1387 (1995)
8. B.S. Kang, J.S. Lee, L. Stan, J.K. Lee, R.F. DePaula, P.N. Arendt et al., *Appl. Phys. Lett.* **85**, 4702 (2004)
9. C.L. Canedy, S. Aggarwal, H. Li, T. Venkatesan, R. Ramesh, F.W. Van Keuls et al., *Appl. Phys. Lett.* **77**, 1523 (2000)
10. A. Vorobiev, P. Rundqvist, K. Khamchance, S. Gevorgian, *J. Euro. Ceram. Soc.* **23**, 2711 (2003)
11. T. Higuchi, Y. Chen, J. Koike, S. Iwashita, M. Ishida, T. Shimoda, *Jpn. J. Appl. Phys.* **41**, 6867 (2002)
12. O. Nakagawa, M. Kobayashi, Y. Yoshino, Y. Katayama, H. Tabata, T. Kawai, *J. Appl. Phys.* **78**, 7226 (1995)
13. H.S. Kim, T.S. Hyun, H.G. Kim, I.D. Kim, T.S. Yoon, J.C. Lee, *Appl. Phys. Lett.* **89**, 052902 (2006)